Supporting Information

Fabrication of superaerophobic Ru-doped *c*-$CoSe_2$ for efficient hydrogen production

Yujie Wei,‡[a] Jianying Wang,‡[b] Yahang Shang,[a] Chang Lv,[a] Xiaoyang He,[b] Tao Wang,[a] Zuofeng Chen,[b] Lvlv Ji[a] and Sheng Wang*[a]*

[a]School of Materials Science and Engineering, Zhejiang Sci-Tech University, Hangzhou 310018, China

[b]School of Chemical Science and Engineering, Tongji University, Shanghai 200092, China

‡These two authors contributed equally to this work.

*Corresponding authors. E-mail addresses: llji@zstu.edu.cn (Lvlv Ji); wangsheng@zstu.edu.cn (Sheng Wang)

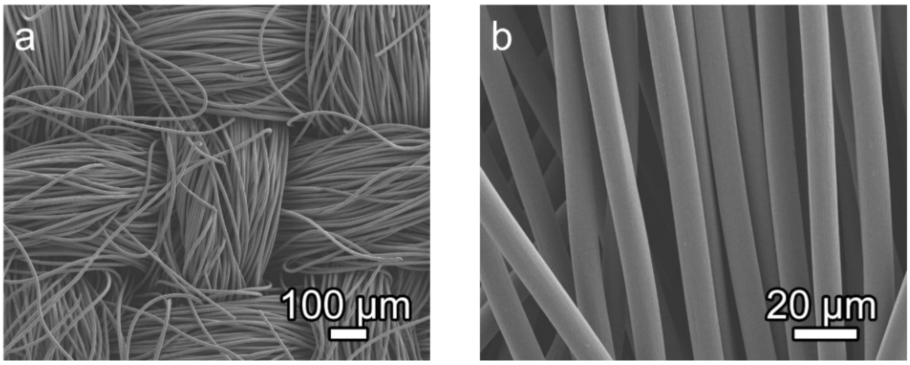

Figure S1. SEM images of CC at different magnifications.

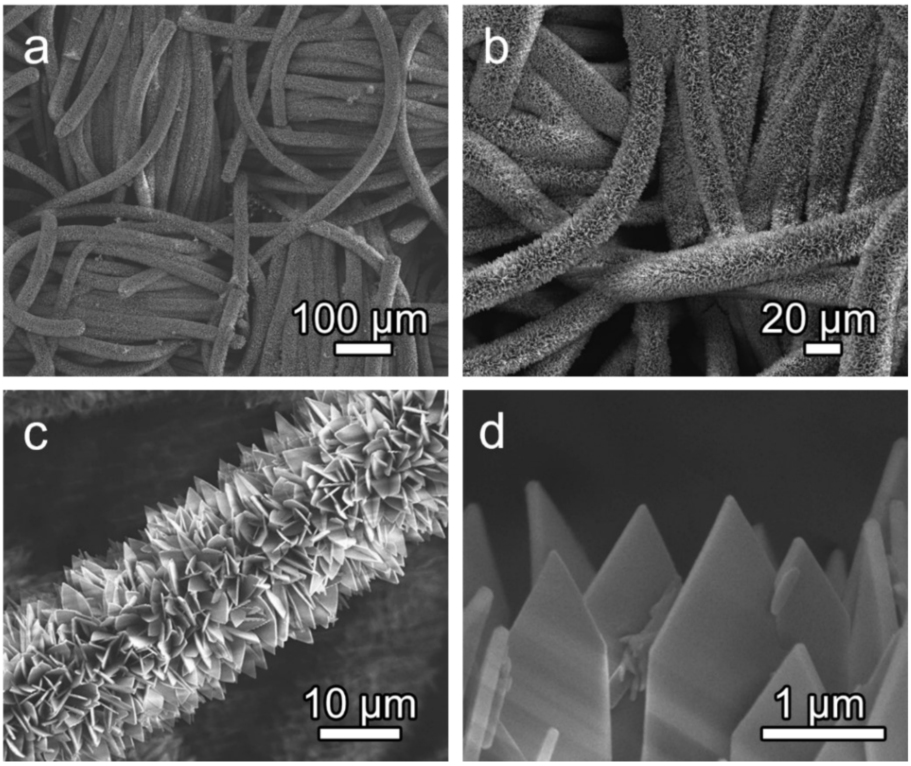

Figure S2. SEM images of Co-ZIF/CC at different magnifications.

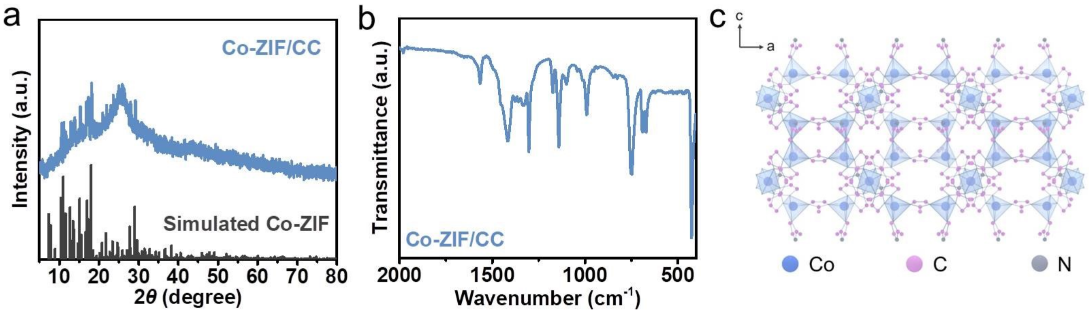

Figure S3. (a) XRD pattern and (b) FT-IR spectrum of Co-ZIF/CC. (c) Crystal structure of Co-ZIF.

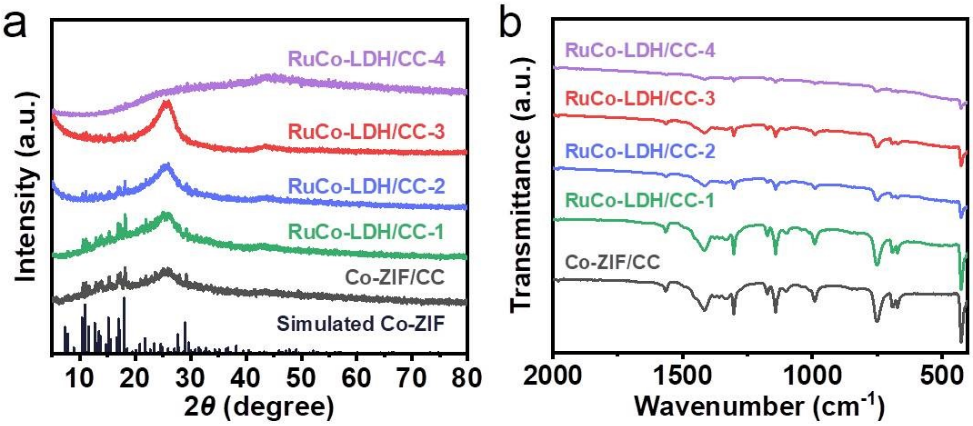

Figure S4. (a) XRD patterns and (b) FT-IR spectra of Co-ZIF/CC and RuCo-LDH/CC-*x* series samples.

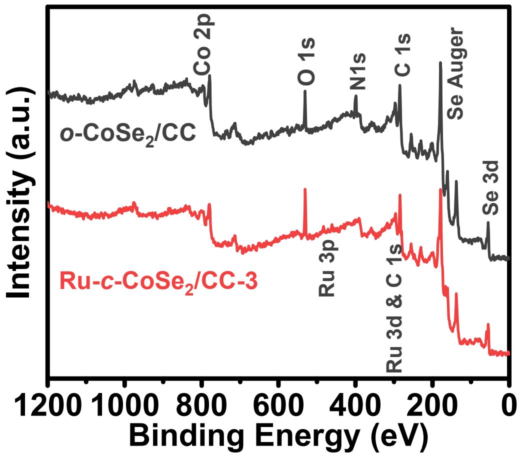

Figure S5. XPS survey spectra of *o*-$CoSe_2$/CC and Ru-*c*-$CoSe_2$/CC-3.

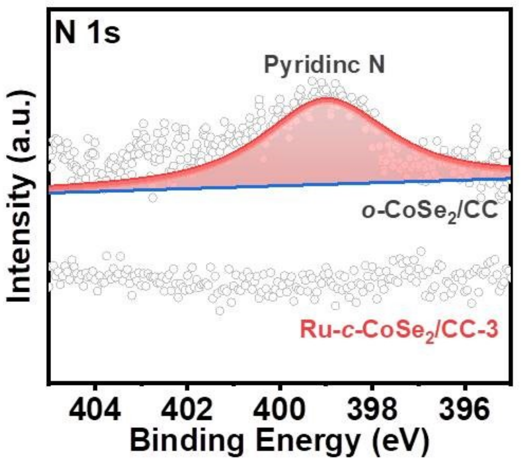

Figure S6. High-resolution N 1s XPS spectra of *o*-$CoSe_2$/CC and Ru-*c*-$CoSe_2$/CC-3.

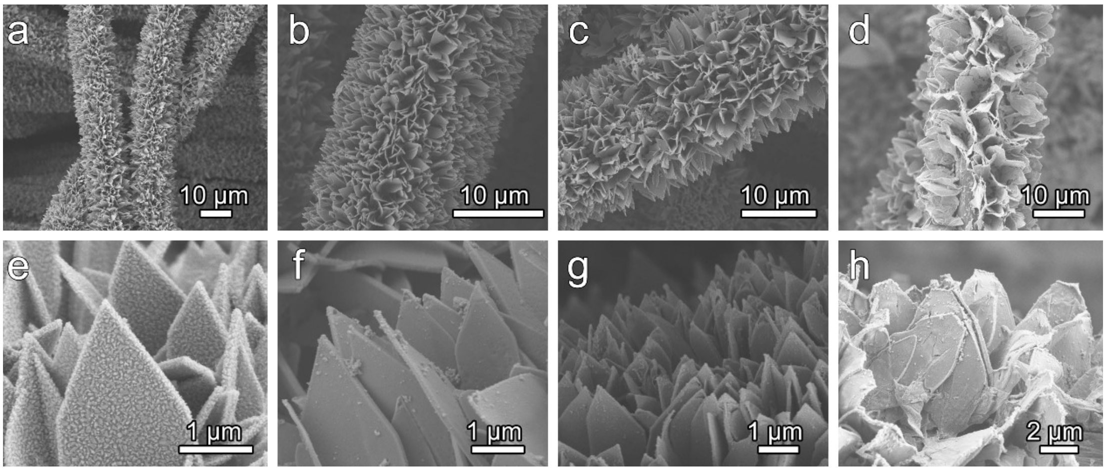

Figure S7. SEM images of (a, e) *o*-$CoSe_2$/CC, (b, f) Ru-*c,o*-$CoSe_2$/CC-1, (c, g) Ru-*c,o*-$CoSe_2$/CC-2, and (d, h) Ru-*c*-$CoSe_2$/CC-4.

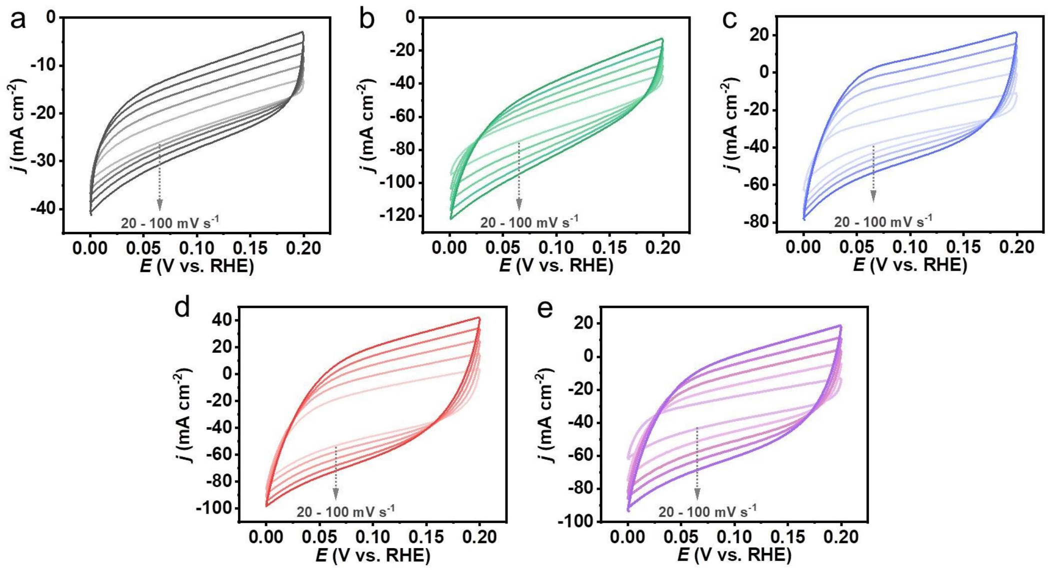

Figure S8. CV curves of (a) *o*-$CoSe_2$/CC, (b) Ru-*c,o*-$CoSe_2$/CC-1, (c) Ru-*c,o*-$CoSe_2$/CC-2, (d) Ru-*c*-$CoSe_2$/CC-3 and (e) Ru-*c*-$CoSe_2$/CC-4 at different scan rates from 20 to 100 mV s^{-1} within the potential range of 0 – 0.2 V vs. RHE in 0.5 M H_2SO_4.

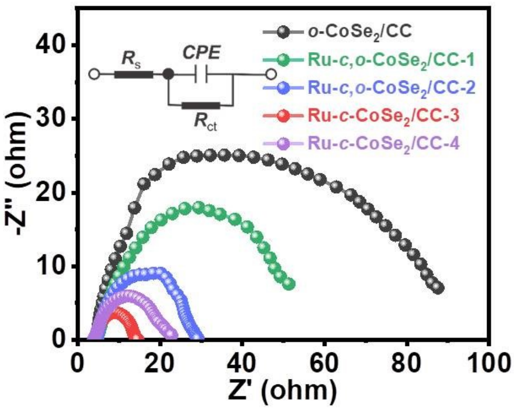

Figure S9. Nyquist plots of the samples in 1 M KOH under an overpotential of 110 mV.

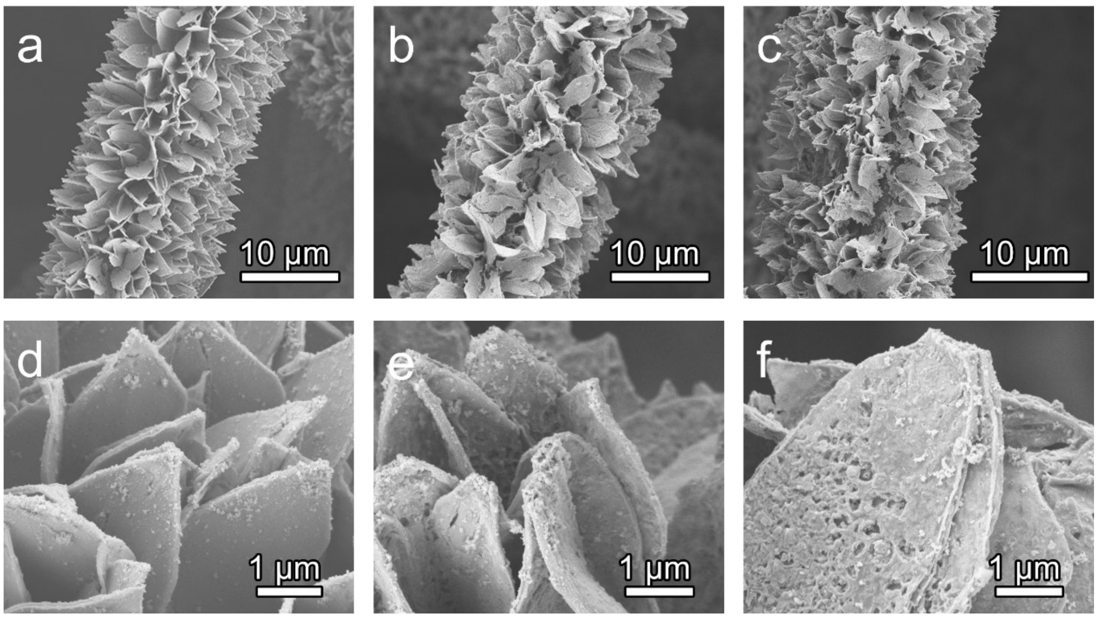

Figure S10. SEM images of (a, d) Ru-*c*-$CoSe_2$/CC-3, (b, e) Ru-*c*-$CoSe_2$/CC-450 and (c, f) Ru-*c*-$CoSe_2$/CC-500.

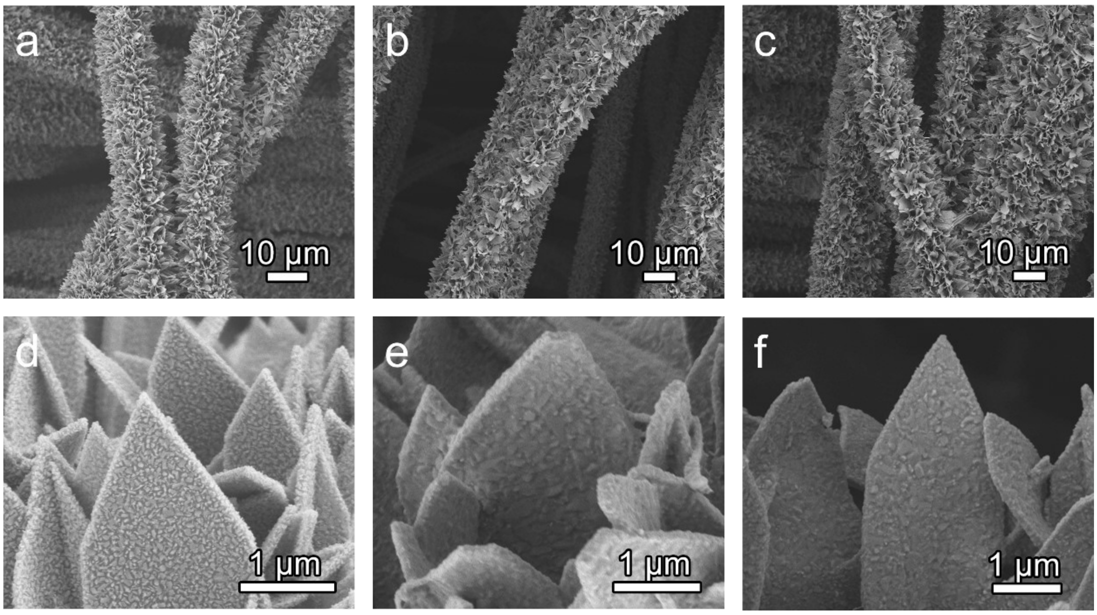

Figure S11. SEM images of (a, d) *o*-$CoSe_2$/CC, (b, e) *c,o*-$CoSe_2$/CC-450 and (c, f) *c*-$CoSe_2$/CC-500.

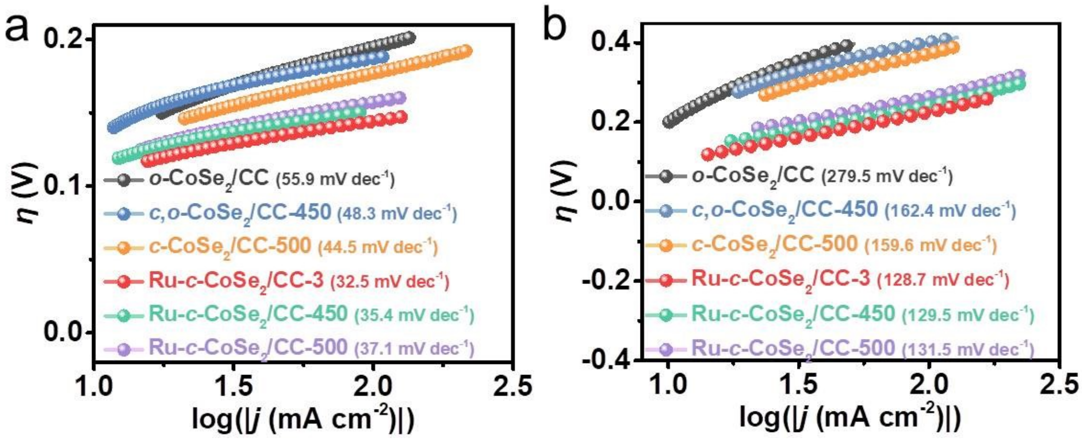

Figure S12. Tafel plots of *o*-$CoSe_2$/CC, *c,o*-$CoSe_2$/CC-450, *c*-$CoSe_2$/CC-500, Ru-*c*-$CoSe_2$/CC-3, Ru-*c*-$CoSe_2$/CC-450 and Ru-*c*-$CoSe_2$/CC-500 in (a) 0.5 M H_2SO_4 and (b) 1 M KOH.

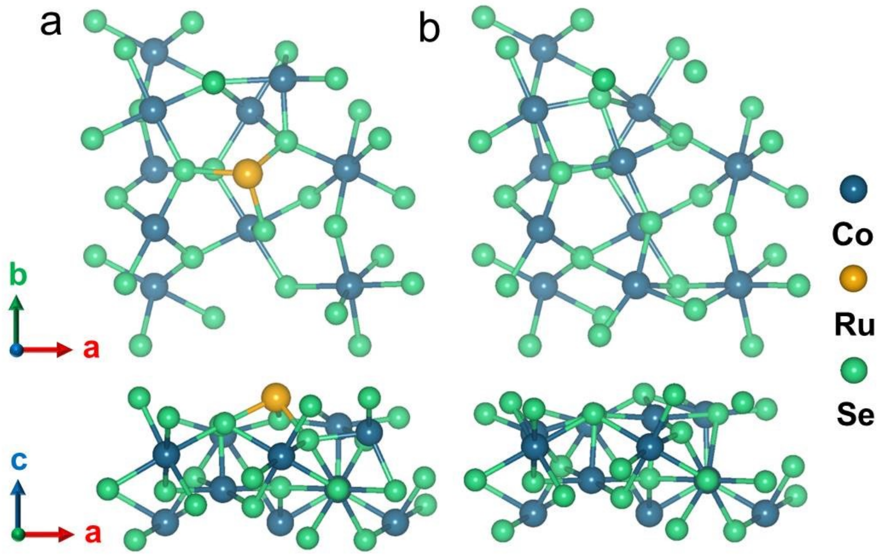

Figure S13. Top and side views of schematic models for (a) Ru-*c*-$CoSe_2$(211) and (b) *c*-$CoSe_2$(211).

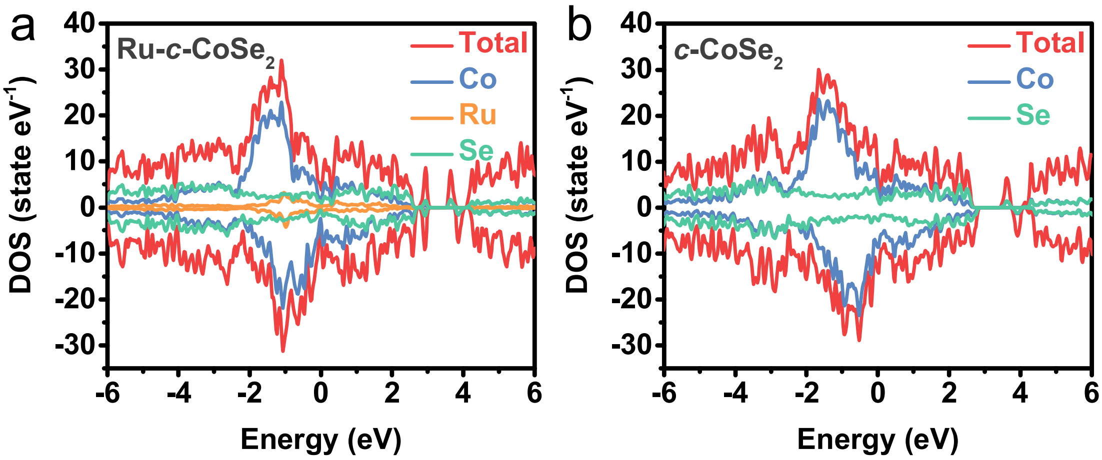

Figure S14. The electronic density of states calculated for (a) Ru-*c*-$CoSe_2$ and (b) *c*-$CoSe_2$.

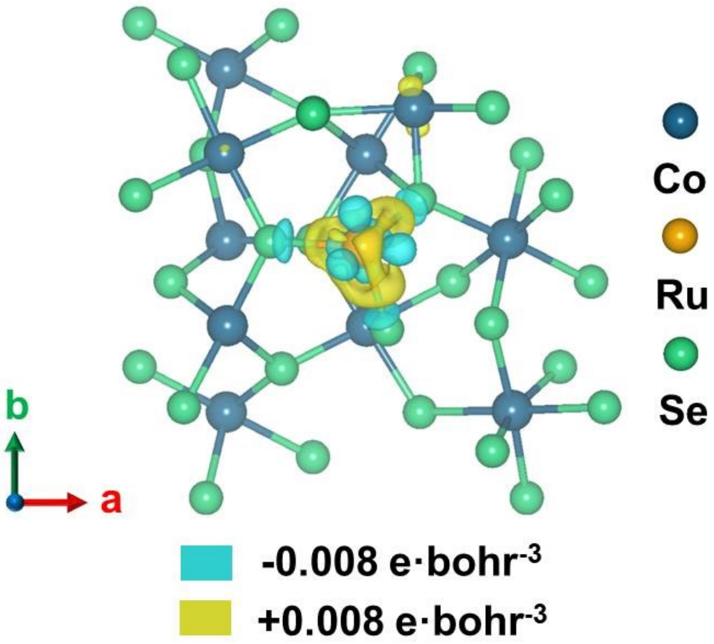

Figure S15. Top view of schematic model of charge density-difference for Ru-*c*-$CoSe_2$.

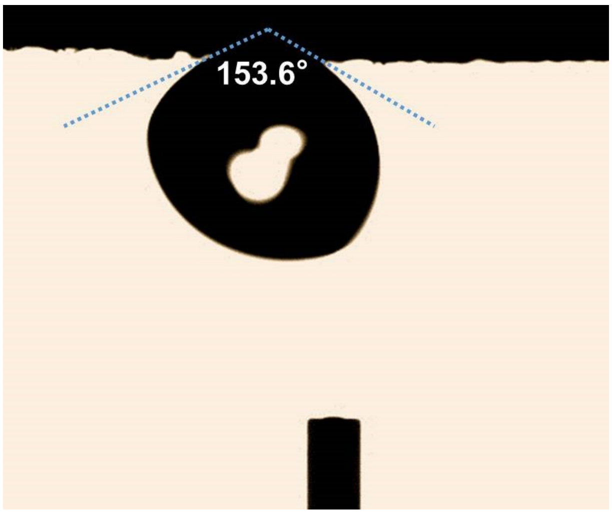

Figure S16. Contact angle of a H_2 bubble on Ru-*c*-$CoSe_2$/CC-3.

Table S1. Comparison of the HER catalytic performance of Ru-*c*-$CoSe_2$/CC-3 with the reported $CoSe_2$-based electrocatalysts in 0.5 M H_2SO_4.

Electrocatalysts	η_{10} (mV)	η_{100} (mV)	b (mV dec^{-1})	Ref.
Ru-c-$CoSe_2$/CC-3	***105***	***144***	***32.5***	***This work***
Fe-$CoSe_2$@NC	143	184	40.9	*ACS Sustain. Chem. Eng.* **2018**, *6*, 8672
$CoSe_2$@DC	132	260	82	*Nano Energy* **2016**, *28*, 143
pure $CoSe_2$	209	-	72.2	*Electrochim. Acta* **2019**, *322*, 134739
m-$CoSe_2$	124	-	60	*Nat. Commun*. **2019**, *10*, 5338
$CoSe_2$/CNTAs-3	204	229	36.7	*Electrochim. Acta* **2018**, *285*, 254
$CoSe_2$/SDGC-60	203	-	55.8	*Int. J. Hydrogen Energy* **2019**, *44*, 13424
$CoSe_2$	115	235	115	*Small* **2020**, *16*, 1906629
o-$CoSe_2$-NC	147	-	39.8	*ACS Sustain. Chem. Eng.* **2022**, *10*, 4022
CoSe	242.8	-	58	*Angew. Chem. Int. Ed.* **2020**, *59*, 22743
c-$CoSe_2$@HC	189.2	-	50.8	*Chem. Eng. J.* **2021**, *424*, 130341
$CoSe_2$ NPs	169	-	56	*J. Mater. Chem. A* **2018**, *6*, 7842
MOF-D $CoSe_2$	195	-	43	*Sustain. Energy Fuels* **2021**, *5*, 4992
$CoSe_2$-CNT	174	-	37.8	*Small* **2017**, *13*, 1700068
1D-$CoSe_2$(tex-48h) nanoarray	216	-	78	*Dalton Trans.* **2020**, *49*, 14191

Table S2. Comparison of the HER catalytic performance of Ru-*c*-$CoSe_2$/CC-3 with the reported $CoSe_2$-based electrocatalysts in 1 M KOH.

Electrocatalysts	η_{10} (mV)	η_{100} (mV)	b (mV dec^{-1})	Ref.
Ru-c-$CoSe_2$/CC-3	***97***	***226***	***128.7***	***This work***
c-$CoSe_2$/CC	190	-	85	*Adv. Mater.* **2016**, *28*, 7527
N-*c*-$CoSe_2$	98	-	63.4	*Angew. Chem. Int. Ed.* **2021**, *60*, 21575
$CoSe_2$/CC	136	380	58	*Chin. Chem. Lett.* **2023**, *34*, 107364
MOF-$CoSe_2$-160°	156	-	40	*Inorg. Chem.* **2020**, *59*, 12778
B-$CoSe_2$/CC	153	260	85	*Colloids Surf. A Physicochem. Eng. Asp.* **2022**, *646*, 128903
Annealled c-$CoSe_2$	248	-	155	*Nat. Commun.* **2018**, *9*, 2533
o-$CoSe_2$	220	-	107	*ACS Omega* **2022**, *7*, 15901
MoS_2@$CoSe_2$-CC	101	-	67	*Nanoscale* **2022**, *14*, 2490
c-$CoSe_2$	149	-	79.1	*J. Mater. Chem. A.* **2017**, *5*, 4513
$CoSe_2$ NPs	278	-	120	*J. Mater. Chem. A.* **2018**, *6*, 7842
o-$CoSe_2$/c-$CoSe_2$/ $MoSe_2$	112	-	96.9	*Mater. Today Chem.* **2022**, *23*, 100724
CoSe/Co(OH_2)-CM(AE)	207	-	126	*Compos. B. Eng.* **2022**, *236*, 109823
$CoSe_2^{(400)}$-NC-800	234	-	95	*ACS Appl. Mater. Interfaces* **2019**, *11*, 3372
p-$CoSe_2$/CC	138	-	83	*ACS Sustain. Chem. Eng.* **2018**, *6*, 15374